Bias-dependent imaging of the In-terminated InAs(001) $(4\times2)/c(8\times2)$ surface by STM: Reconstruction and transitional defect

C. Kendrick
Department of Electrical Engineering, Princeton University, Princeton, New Jersey 08544

G. LeLay
Centre de Recherche sur les Mécanismes de la Croissance Cristalline–CNRS, Campus de Luminy, Case 913, F-13288 Marseille Cedex 9, France

A. Kahn
Department of Electrical Engineering, Princeton University, Princeton, New Jersey 08544

(Received 7 June 1996)

We use low-energy electron diffraction (LEED) and scanning tunneling microscopy (STM) to study the In-terminated InAs(001) surface prepared by argon sputtering and annealing. Characterization by LEED shows the formation of a highly ordered surface with a mixture of (4×2) and $c(8\times2)$ phases. We systematically vary the sample bias in STM to obtain bias-dependent images over the same surface regions, allowing discrimination between topographic and electronic features. Atomic resolution STM images confirm the existence of both (4×2) and $c(8\times2)$ phases and identify an electronic signature at the transition between the two reconstructions. Images of (4×2) regions are consistent with a previously proposed model for this surface in which the unit cell contains one In dimer in the first layer and two In dimers in the third layer. The $c(8\times2)$ reconstruction, though similar to the (4×2), is found to arise from a shift in the third- and/or first-layer In dimers by one lattice spacing. Filled-state imaging at the (4×2)-to-$c(8\times2)$ boundary shows two bright spots positioned midway between the first-layer In dimer rows. In empty states, these spots are entirely absent, underlining their electronic origin. These electronic features are explained in terms of a localization of charge due either to a structural defect or to the presence of a sulfur doping atom at the transition from (4×2) to $c(8\times2)$ reconstructions. [S0163-1829(96)09548-3]

I. INTRODUCTION

Scanning tunneling microscopy (STM) has made great contributions to the determination of reconstructions and atomic configurations at the surfaces of semiconductors. STM has been especially illuminating in studies of polar surfaces of III-V semiconductors which exhibit complex reconstructions with large unit cells composed of surface-atom dimers and vacancies, for example, the As-[1–3] and Ga-terminated[4,5] GaAs(100) surfaces. Throughout this process, the justification of structures based on the electron counting rule[6] has been quite successful. Recently, the polar surfaces of many other III-V materials, in particular the low-band-gap semiconductors InSb (Ref. 7) and InAs,[8,9] have been investigated with STM. As with GaAs(100), the principles of electron counting in combination with STM have led to considerable progress in the determination of the surface atomic arrangement of these materials.

Several instances exist where STM, used in the spectroscopic mode, has also been successful in detecting localized charges at semiconductor surfaces and identifying their origin. Highly electronegative adsorbates on clean GaAs(100) surfaces[10] have been shown to locally trap electrons. Both acceptor and donor ionized dopant impurities have been found to modify the local electronic potential at the GaAs(110) surface.[11] STM has shown charge trapping at kink sites on GaAs(100) (2×4) that act as a Fermi-level pinning mechanism and serve to compensate the Si-doped bulk.[12]

In the present study, we use both the microscopic and spectroscopic aspects of STM to investigate the In-terminated InAs(001) surface. It is well known that at several InAs surfaces [(111),[13] $(\overline{1}\overline{1}\overline{1})$,[13] (110),[14] and As-terminated (100) (Refs. 13,15) the Fermi level (E_F) is located up to 0.2 eV above the conduction-band minimum, leading to the formation of an electron accumulation layer with an approximate charge density of $\sim1\times10^{12}$ cm^{-2}.[13,15] However, studies have also shown that only a weak accumulation layer is formed on the In-terminated InAs(001) (4×2) surface. Measurements by high-resolution electron-energy-loss spectroscopy determined the accumulated electron density to be $<5\times10^{11}$ cm^{-2},[15] while angle-resolved ultraviolet photoemission spectroscopy found E_F to be positioned closely below the conduction-band minimum.[13] Despite the growing number of studies on this phenomenon, the exact origin of E_F pinning within the conduction band remains controversial. By studying the clean InAs(001) (4×2) surface with STM, we hope to gain a better understanding of the mechanisms which lead to electron accumulation at some InAs surfaces but not at others. We investigate the structure of the InAs(001) $(4\times2)/c(8\times2)$ surface and discriminate between features of topographic versus electronic origin by comparing filled- and empty-state

STM images. We obtain atomic-resolution images which point out distinct (4×2) and $c(8\times2)$ surface regions and support the structural model proposed by Ohkouchi and Ikoma.[8] In addition, we find an electronic signature at the transition between the two structures that is associated with the localization of negative charge.

II. EXPERIMENTAL DETAILS

All experiments were performed in a single ultrahigh vacuum (UHV) system consisting of load lock, analysis, and STM chambers. Base pressures in the analysis and STM chambers were $\sim1\times10^{-10}$ and $\sim6\times10^{-11}$ Torr, respectively. The analysis chamber is equipped with Auger electron spectroscopy (AES), low-energy electron diffraction (LEED), argon ion sputtering, and sample heating. Highly doped *n*-type InAs(001) samples (sulfur, $n=2.3\times10^{17}$ cm^{-3}) with a miscut of $\pm0.5°$ were inserted into the analysis chamber via the load lock after a degreasing procedure of sequential trichloroethylene, acetone, and methanol baths. These samples were degassed at ~250 °C for 1 h to remove excess contamination before surface preparation. Cycles of argon ion sputtering and annealing (ISA) were performed to prepare the InAs(001) surfaces. Sputtering cycles lasting 15 min at energies of 500 eV or 1 keV were used while keeping the substrate temperature at ~300 °C until no carbon or oxygen could be detected by AES. The samples were then annealed for ~1 h to 420–480°C as determined by an infrared pyrometer while maintaining the chamber pressure below $\sim2\times10^{-9}$ Torr. Subsequent to the annealing, no carbon or oxygen was present as measured by AES. The surface symmetry was then determined by LEED and the samples were transferred to the STM chamber for characterization.

We use a home-built UHV-STM based on the design of Demuth *et al.*,[16] with the added capability of stable operation at tunneling currents as low as 15 pA. STM tips were formed by electrochemical etching of tungsten wire in 2-M potassium hydroxide and heated in vacuum by electron bombardment to above 800 °C for 15–20 min. The tunneling current of images presented in this paper varied between 100 and 400 pA for resolution optimization depending on particular tip and/or surface conditions. The sample bias was systematically varied to probe filled states in the valence band as well as empty states of the conduction band, in an effort to separate surface electronic features from topographic features. Filled- and empty-state images were recorded sequentially, rather than simultaneously.

III. RESULTS

A typical LEED pattern for InAs(001) following an annealing at 420 °C is shown in Fig. 1. The fourth-order spots are very sharp and the background intensity is low, indicating a highly ordered, smooth surface with a large coherence length within the reconstructed areas. While there is some streaking of the twofold spots in the $[\bar{1}10]$ direction, two spots exhibiting eightfold periodicity are clearly visible. It is therefore reasonable to expect a surface structure composed of both (4×2) and $c(8\times2)$ phases.

A large area STM scan of filled states is shown in Fig. 2. The surface exhibits large flat terraces generally ~500 Å in width, which is consistent with the angle of miscut and with the sharp LEED pattern of Fig. 1. Even on this large scale image, the $4\times$ periodicity along $[\bar{1}10]$ is evident. It consists of long, unkinked lines along the $[110]$ direction within which the $2\times$ periodicity is not resolved at this magnification. InSb(100) surfaces prepared by cycles of ISA also exhibit well-ordered structures over such large distances (~1000 Å),[17] and this seems to be a general trend of low band-gap materials. We have also observed STM images showing a low coverage of small clusters (50–100 Å in diameter), presumably composed of In, which may be due to the effect of slightly higher annealing temperatures and/or preferential sputtering of surface In.[7] Samples annealed to ~480 °C show more pronounced signs of In clustering by a slight ''clouding'' of the mirrorlike surface upon visual inspection. STM on such samples show crystallites ~1500 Å

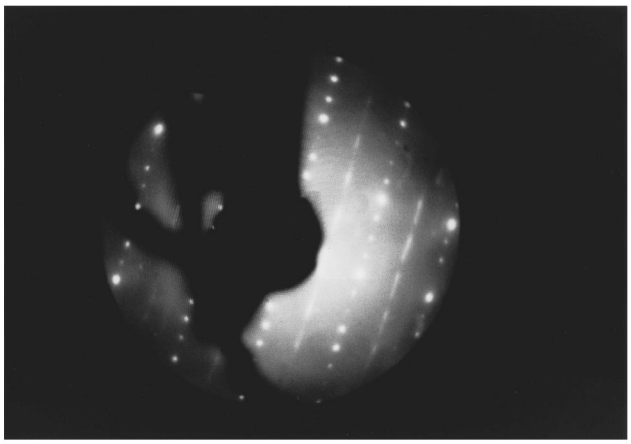

FIG. 1. (4×2)-$c(8\times2)$ LEED pattern ($E_p=44$ eV) obtained from an InAs(001) sample prepared by ion sputtering and annealing at ~420 °C. Though the $2\times$ structure is streaked, an $8\times$ periodicity is clearly shown in the far right of the pattern.

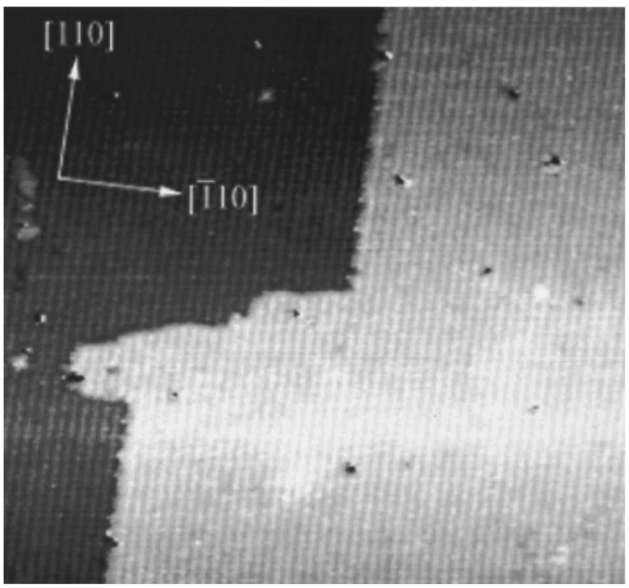

FIG. 2. 1000 Å $\times$1000 Å filled-state STM image ($V_s=-1.0$ V) of the clean (4×2) $c(8\times2)$ InAs(001) surface. The unkinked vertical-line structure shows the $4\times$ periodicity (17.2 Å).

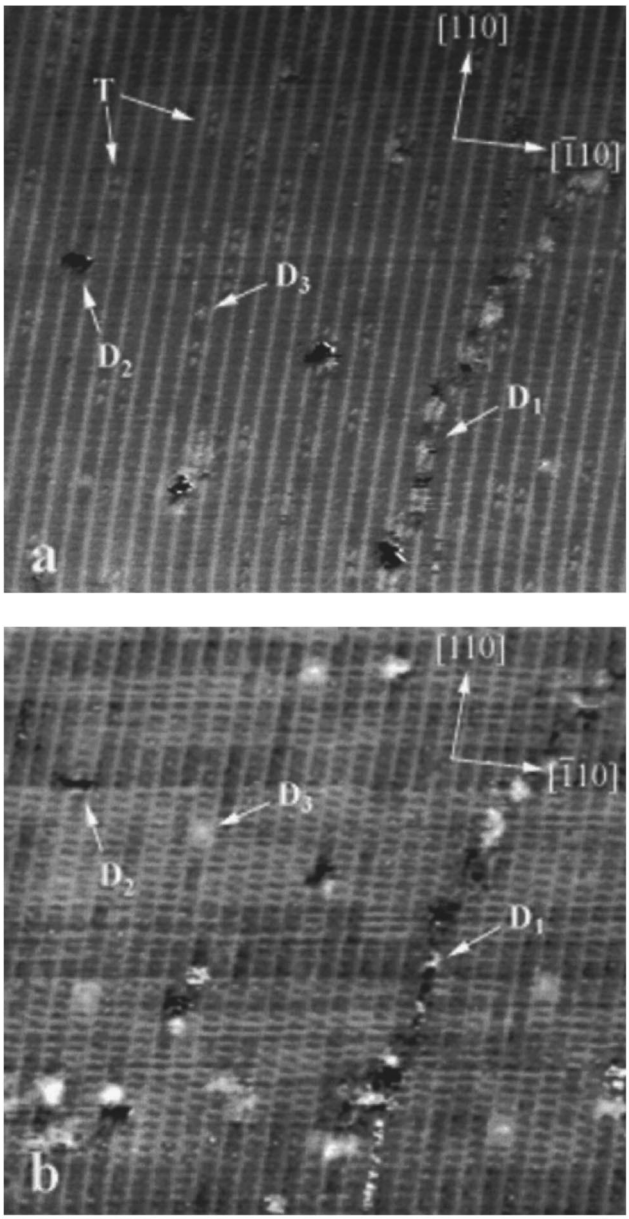

FIG. 3. Topographic features are discriminated from electronic features by observing filled- (a) and empty- (b) state images. D_1 is a dislocation line across which periodicity shifts by the $2\times$ distance, while D_2 and D_3 are topographic depressions and protrusions, respectively [500 Å $\times$500 Å: (a) $V_s=-800$ mV; (b) $V_s=+900$ mV].

in diameter with a well-defined orientation with respect to the substrate. We note that the very smooth morphology and high degree of ordering of the ISA-prepared surfaces are in contrast to the highest quality Ga-terminated GaAs(100) (4×2) surfaces prepared by molecular beam epitaxy.[4,5] Island structures give the GaAs(100) (4×2) surface a roughness of at least three terrace layers ($\sim$8.4 Å). In that context, it is interesting to note that small amounts of In present on GaAs(100) have been shown to improve surface ordering and morphology,[18] implying that In termination may be more energetically stable than Ga, As, or Sb termination.

In Figs. 3(a) and 3(b) we show smaller scale filled- and empty-state STM images, respectively. As the sample bias is progressively decreased (in an absolute sense), states closer to the valence-band maximum and conduction-band minimum are probed. The STM image contrast under these conditions tends to increase, making the $4\times$ periodic lines narrower and showing the emergence of a $2\times$ periodic ladder structure. Several other features in these images deserve mention. First, a surface dislocation line D_1 is seen extending from the upper right to the bottom edge of the image across which the periodicity shifts by $\frac{1}{2}$ in the [$\bar{1}$10] direction. Dislocation lines having $\frac{1}{4}$ periodicity shifts have also been observed and, together with other structural features, help to elucidate the atomic arrangement of the reconstructed phases. Second, there appear defects D_2 and D_3, which are confirmed to be topographic depressions and protrusions by imaging the same area in filled and empty states. These features are very useful in comparing images acquired consecutively with various sample biases, since they remain fixed and relatively insensitive to bias changes. Note that the filled-state features T, consisting of a pair of bright spots located between the $4\times$ periodic rows, are entirely absent in the empty-state image. We have observed surfaces immediately following preparation as well as after $\sim$1 week in vacuum and found roughly the same density of T features $\pm10\%$. Thus we can rule out contamination from residual gas species as being responsible for these features. It will be shown that T is a defect which is always associated with the transition between (4×2) and $c(8\times2)$ phases. We defer this discussion until after the ideal surface structure is presented.

IV. DISCUSSION

A. The $(4\times2)/c(8\times2)$ structure

Figures 4(a) and 4(b) show filled- and empty-state STM images, respectively, taken over the same surface area with defect D_3 serving as a common reference point. Since the brighter, narrow rows along the [110] direction in Figs. 4(a) and 4(b) have the same registry with respect to defect D_3, the rows are attributed to a topographic feature. Figure 4(b) shows an atomic resolution image where the twofold periodicity is clear and which enables the specific determination of (4×2) versus $c(8\times2)$ unit cells (outlined). The measured unit cell dimensions are in good agreement with the expected $4\times$ distance (17.2 Å) and $2\times$ distance (8.6 Å). Again, it is noted that the transitional defects T, mentioned above and shown in Fig. 4(a), do not appear in Fig. 4(b).

A structural model of the atomic bonding for the (4×2) structure has been proposed[8] and is presented here in the upper part of Fig. 5. This model has a unit cell consisting of one In dimer in the first layer and two In dimers in the third layer. It explains well the (4×2) symmetry as observed by LEED and can be shown to satisfy the electron counting rule. The fact that STM shows the bright rows to be topographic features agrees with the large height corrugation (3 Å) between the first- and third-layer In dimers. We attribute the maxima spaced by the $2\times$ distance along the bright rows of Fig. 4(b) to tunneling into the empty dangling bonds (DB's) of the first-layer In dimers. Conversely, the bright rows seen in filled-state images [Fig. 4(a)] are attributed to a combination of tunneling out of the first layer In dimer bonds and the

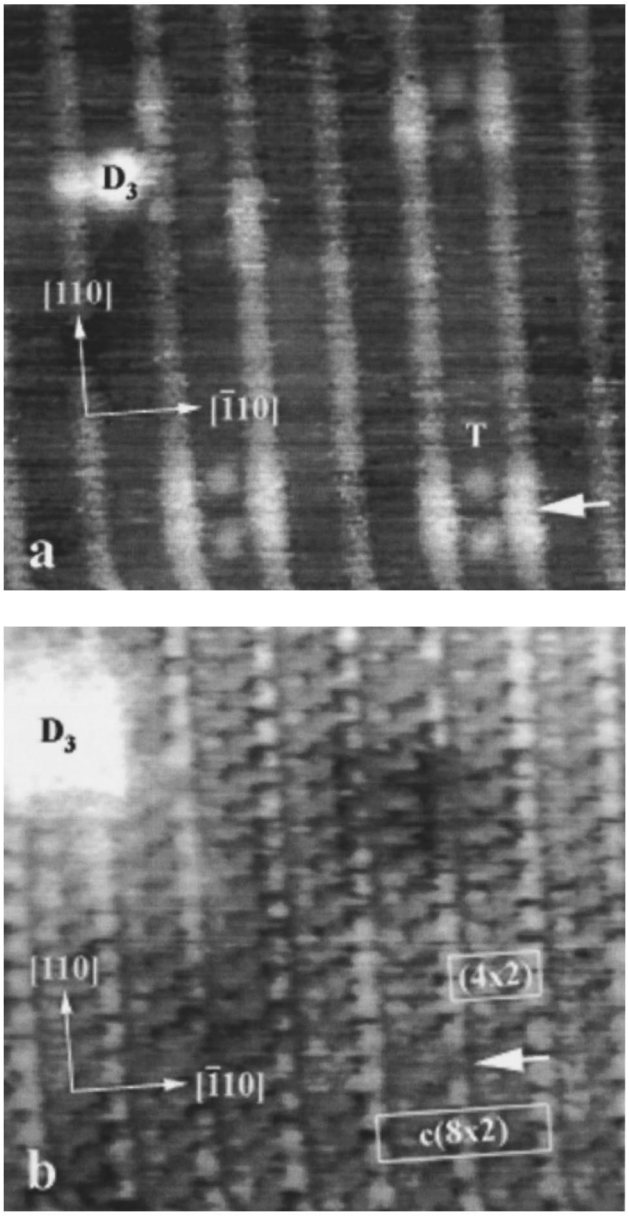

FIG. 4. Filled- (a) and empty- (b) state images of the same surface area using defect D_3 as a common reference point. Atomic resolution of (b) enables determination of separate (4×2) and $c(8\times2)$ regions (unit cells outlined). Large white arrow indicates the position of an In-atom vacancy within the first layer [120 Å $\times$120 Å: (a) $V_s=-600$ mV; (b) $V_s=+350$ mV].

second-layer As filled DB's. The filled-state intensity in between the bright rows in Fig. 4(a) is weak; however, images acquired under different bias voltages clearly show a structure of two equally spaced lines along the [110] direction, which appear dashed in the highest resolution images [see Fig. 6(a)]. The empty-state intensity, better seen in Figs. 6(b) and 7(b), are attributed to empty DB states of the third-layer In dimers. All of these results strongly support the validity of the (4×2) model presented by Ohkouchi and Ikoma.[8]

The $c(8\times2)$ phase can be formed in a variety of ways, all of which satisfy the electron counting rule. The simplest is shown in the lower portion of Fig. 5, where the grayed region spans a $3\times$ distance. By spacing the third-layer In dimers by an *odd* interval, the third-layer structure in adjoining unit cells is no longer aligned but staggered, forming the larger $c(8\times2)$ unit cell. Alternately, the $c(8\times2)$ can be formed by removing one In atom from a first-layer In dimer in a (4×2) reconstructed region. The first-layer In atoms are then allowed to redimerize along the [110] direction, leaving a vacancy within the first-layer In dimer row and shifting periodicity by one lattice spacing. This type of defect is identified by the large white arrow in Fig. 4(b). Of course, both of the defects just described could occur together and, in fact, this occurs in all of the transitional defects shown in Figs. 4(a) and 4(b). It is difficult to estimate the frequency of occurrence of each type of transitional defect due to variability in STM resolution. Unfortunately, image resolution sufficient to resolve the difference between (4×2) and $c(8\times2)$ regions usually occurs only in either the first layer *or* the third layer, but generally not in both. However, in every case in which T appears, empty-state images show a $3\times$ spacing within the third layer, regardless of the first-layer In dimer structure. Therefore, it is believed that the appearance of T is due only to the structure of the defect within the third layer.

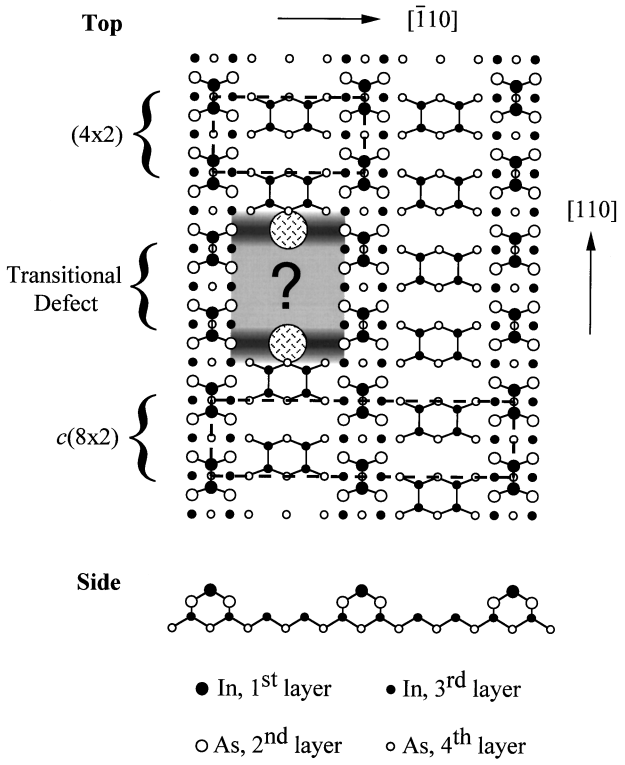

FIG. 5. Schematic atomic model showing the (4×2) reconstruction, the $c(8\times2)$ reconstruction, and the transitional defect. In the defect region, empty-state intensity is shown as shaded, whereas filled-state intensity is represented by hatched circles.

B. The transitional defect "*T*"

We now return to feature T, the two bright spots that appear only in filled-state images and that are always present at the transition between (4×2) and $c(8\times2)$ phases. Such a bias-dependent behavior is indicative of a localized charge state and has been reported in several other studies.[9–12] In the present case, feature T appears to be an acceptor state, trap-

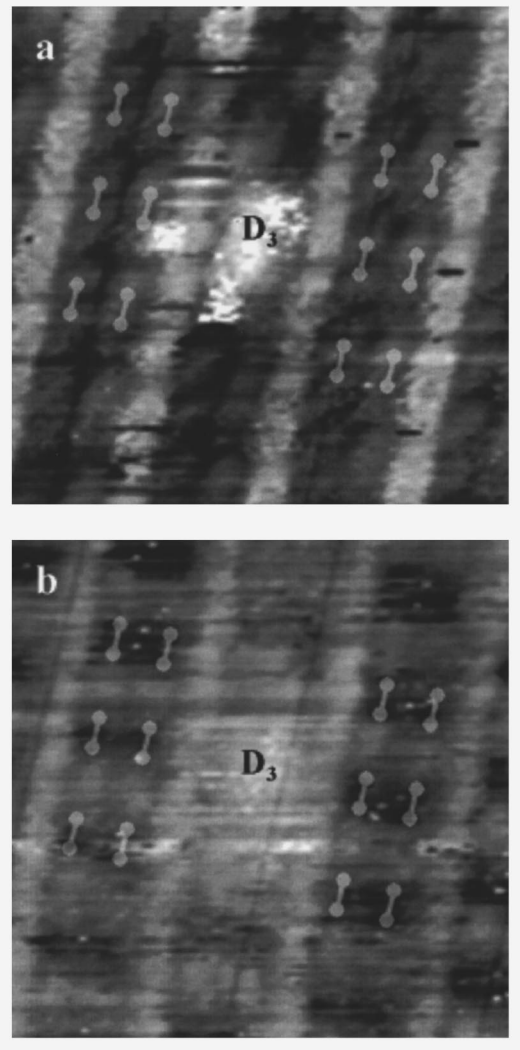

FIG. 6. Complementary behavior of STM intensity in filled (a) and empty (b) states is observed in relation to the same topographic defect of type D_3 (60 Å $\times$60 Å: (a) $V_s=-600$ mV; (b) $V_s=+1.0$ V).

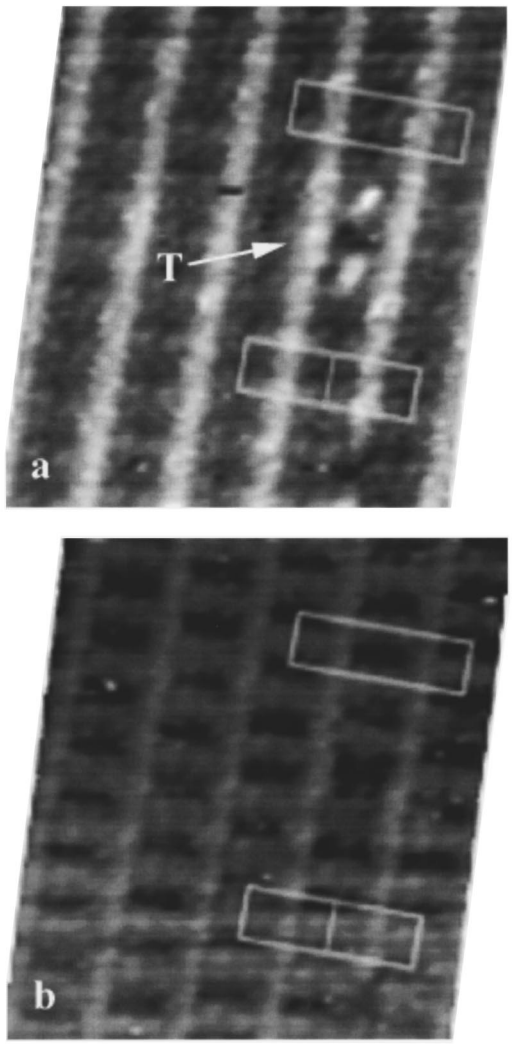

FIG. 7. Filled- (a) and empty- (b) state images of the same isolated transitional defect. Boxes are placed at the same surface position in each image, outlining $c(8\times2)$ and (4×2) unit cells above and below T, respectively. The intensity maxima of T in (a) are at the same position as the $3\times$-spaced intensities of the third layer in (b) (80 Å $\times$80 Å: (a) $V_s=-700$ mV; (b) $V_s=+900$ mV).

ping a small amount of negative charge at or near the surface. This is similar to the compensating surface defects that have been reported for GaAs(100) (2×4) induced by high-density Si doping.[12]

It is worth noting that the bright spots of T are spaced by a $3\times$ distance (12.4 Å), the same distance that appears between third-layer intensity maxima at the same position in empty-state images [seen more clearly in Figs. 7(a) and 7(b)]. One may guess that the spots are in exactly the same position as the empty-state $3\times$ intensity by simply relying on symmetry arguments. However, because the STM images presented here are acquired consecutively, we cannot rule out a shift of T relative to the empty-state intensity based solely on this argument. In order to determine the precise position of T with respect to the actual atomic positions, it is necessary to consider the nature of STM contrast when imaging either filled or empty states.

It is reasonable to presume, and total-energy calculations have confirmed,[5] that filled-state STM images more closely follow topographic contours. This can be understood in terms of tunneling out of the filled bonds that hold together surface dimers. Since it is known that the bright rows along the [110] direction are due to topography (first-layer In dimers), it may be tempting to assign the observed third-layer intensity of both filled- and empty-state images to topographic features as well. Figures 6(a) and 6(b) show this to be false. We show filled- and empty-state images of the same surface area which contains a defect of type D_3. It is clear that the third-layer intensities in Figs. 6(a) and 6(b) are complementary when their positions are referenced to D_3. That is, the third-layer structure which is bright in Fig. 6(a) is dark in Fig. 6(b). Knowing that filled-state image intensity more closely corresponds to atomic positions, we assign the likely positions of In dimers within the third layer as shown in Figs. 6(a) and 6(b).

Within this interpretation, STM image contrast of filled states arises from bonds between atoms as well as from filled DB's. Conversely, STM image contrast of empty states is due to the presence of empty DB's. This picture is fully consistent with the models of (4×2) and $c(8\times2)$ reconstructions already presented in Fig. 5. Furthermore, we now

know the positions of both the third-layer In dimers and their corresponding empty DB's. We may now precisely determine the position of feature *T* with respect to the third-layer dimer positions. Figures 7(a) and 7(b) show filled- and empty-state images of the same isolated transitional defect. The unit cells outlined above and below the defect are positioned by direct computer-aided superposition of Figs. 7(a) and 7(b), with careful compensation for drift between STM scans. This superposition technique shows excellent agreement with filled- and empty-state complementarity, as illustrated in Fig. 6. Using the outlined unit cells as a reference, we find that the two filled-state bright spots of feature *T* [Fig. 7(a)] are at the same position as the $3\times$-spaced empty-state intensity [Fig. 7(b)]. This implies that at these positions there are *either* separate filled and empty states *or* that there is a partially filled surface state. The situation is shown schematically in the grayed region of Fig. 5, where the horizontal shaded bands represent empty states and the hatched circles represent filled states. Although we are unable to determine the exact atomic structure within the gray area of Fig. 5, we discuss two possible origins for the transitional defect.

As mentioned previously, In forms small clusters in low coverage on these sputtered and annealed surfaces, with increasing clustering occurring at higher temperatures. It is not unreasonable to assume that As is not stable under these preparation conditions and that if second-layer As atoms are exposed by an In-atom vacancy in the first layer, they will leave the surface. Because As will desorb once an In-atom vacancy is created in the first layer, it is impossible for that In to regain its initial position. In then tends to accumulate in excess between the first-layer dimer rows. At elevated temperatures and over prolonged periods, a cation antisite (In on an As site) within the third layer could be formed, giving rise to the observed feature *T*. The resulting electronic signature of the defect could be similar in nature to that of the anion antisite defect observed on low-temperature-grown GaAs(100) and observed with cross-sectional STM.[19] Another possibility is the formation of a structure composed of twofold-coordinated In atoms in an $(s+p_z)$ hybridization that have one DB filled and the other empty. Such a situation is believed to occur on the GaAs $(\overline{1}11)$ $(\sqrt{19}\times\sqrt{19})$ reconstruction.[20]

A second possible origin for *T* is the presence of sulfur (the doping element in our samples) at or near the surface. By simply counting the number of transitional defects occurring in a well-defined area we may arrive at an approximate surface density. We find $\sim 1.6\times 10^{12}$ defects/cm^2 on surfaces prepared by ISA, corresponding to a coverage of ~ 0.25 % ML. With a sulfur doping of $n=2.3\times 10^{17}$ cm^{-3}, we expect a surface sulfur density of 3.75×10^{11} cm^{-2}, slightly lower than the observed value. The difference may be accounted for by the well-known phenomenon of impurity diffusion in semiconductors, with enhanced diffusion of impurities occurring along bulk imperfections such as dislocations.[21] Since we indeed observe *T* to decorate the sides of dislocation lines, with one spot appearing on either side of the dislocation, one could argue that sulfur has segregated from the bulk to the surface along so-called ''pipe dislocations.'' Although we have no knowledge of S-diffusion studies in InAs, high S doping in InP is reported to result in a lower dislocation density but with increased decoration as measured by transmission electron microscopy,[22] and similar behavior may be expected from InAs.

Many defect models were explored in this work; however, none were found to satisfy all of the observed features. Future work on this defect should result in a structure having the observed acceptor-state character and symmetry requirements of filled- and empty-state intensities while explaining the transition between (4×2) and $c(8\times 2)$ structures.

V. SUMMARY

We have investigated the (4×2) and $c(8\times 2)$ reconstructions of In-terminated InAs(001) surface prepared by ion sputtering and annealing. LEED and STM show a very smooth and well-ordered surface with wide terraces (>500 Å) across which unkinked dimer rows extend over large distances. Through bias-dependent atomic-resolution imaging, we distinguish electronic from topographic features. We find that the (4×2) reconstruction is compatible with the one In-dimer, three missing In-dimer model proposed by Ohkouchi and Ikoma,[8] and that the $c(8\times 2)$ reconstruction is formed from the (4×2) by shifting the first- and/or third-layer In dimers by one lattice spacing. We observe a feature consisting of two bright spots which appears only in filled-state imaging and which corresponds to a localized acceptor defect state associated with the (4×2)-to-$c(8\times 2)$ transition. By mapping filled- and empty-state intensities in the first and third In-dimer layers, we precisely determine the position of this transitional defect. Its exact structure, however, remains unknown at this time. Possible origins of the defects, e.g., the presence of excess In or a sulfur dopant atom, are discussed.

ACKNOWLEDGMENTS

Support of this work by a grant of the National Science Foundation (No. DMR-93-21826) is gratefully acknowledged. We thank Professor C. Palmstrøm for generously providing us with highly doped InAs(001) substrates, and Dr. D. J. Chadi for very helpful discussions.

[1] M. D. Pashley, K. W. Haberern, W. Friday, J. M. Woodall, and P. D. Kirchner, Phys. Rev. Lett. **60**, 2176 (1988).

[2] D. K. Biegelsen, R. D. Bringans, J. E. Northrup, and L.-E. Swartz, Phys. Rev. B **41**, 5701 (1990).

[3] T. Hashizume, Q. K. Xue, J. Zhou, A. Ichimiya, and T. Sakurai, Phys. Rev. Lett. **73**, 2208 (1994).

[4] S. L. Skala, J. S. Hubacek, J. R. Tucker, J. W. Lyding, S. T. Chou, and K.-Y. Cheng, Phys. Rev. B **48**, 9138 (1993).

[5] Q. Xue, T. Hashizume, J. M. Zhou, T. Sakata, T. Ohno, and T. Sakurai, Phys. Rev. Lett. **74**, 3177 (1995).

[6] M. D. Pashley, Phys. Rev. B **40**, 10 481 (1989).

[7] C. F. McConville, T. S. Jones, F. M. Leibsle, S. M. Driver, T. C.

Q. Noakes, M. O. Schweitzer, and N. V. Richardson, Phys. Rev. B **50**, 14 965 (1994).
[8] S. Ohkouchi and N. Ikoma, Jpn. J. Appl. Phys. **33**, 3710 (1994).
[9] S. Ohkouchi, N. Ikoma, and I. Tanaka, J. Vac. Sci. Technol. B **12**, 2033 (1994).
[10] J. A. Stroscio and R. M. Feenstra, J. Vac. Sci. Technol. B **6**, 1472 (1988).
[11] M. B. Johnson, O. Albreksten, R. M. Feenstra, and H. W. M. Salemink, Appl. Phys. Lett. **63**, 2923 (1993).
[12] M. D. Pashley and K. W. Haberern, Phys. Rev. Lett. **67**, 2697 (1991).
[13] L. Ölsson, C. B. M. Andersson, M. C. Håkansson, J. Kanski, L. Ilver, and U. O. Karlsson (unpublished).
[14] G. LeLay, V. Yu. Aristov, J. Kanski, P. O. Nilsson, U. O. Karlsson, K. Hricovini, and J. E. Bonnet, Appl. Surf. Sci. **70/71**, 502 (1993).
[15] M. Noguchi, K. Hirakawa, and T. Ikoma, Phys. Rev. Lett. **66**, 2243 (1991).
[16] J. E. Demuth, R. J. Hamers, R. M. Tromp, and M. E. Welland, J. Vac. Sci. Technol. A **4**, 1320 (1986).
[17] M. O. Schweitzer, F. M. Leibsle, T. S. Jones, C. F. McConville, and N. V. Richardson, Surf. Sci. **280**, 63 (1993).
[18] U. Resch-Esser, N. Esser, C. Springer, J. Zegenhagen, W. Richter, M. Cardona, and B. O. Firmland, J. Vac. Sci. Technol. B **13**, 1672 (1995).
[19] R. M. Feenstra, J. M. Woodall, and G. D. Pettit, Phys. Rev. Lett. **71**, 1176 (1993).
[20] D. K. Biegelsen, R. D. Bringans, J. E. Northrup, and L.-E. Swartz, Phys. Rev. Lett. **65**, 452 (1990).
[21] E. F. Schubert, *Doping in III-V Semiconductors* (Cambridge University Press, Cambridge, 1993), p. 325.
[22] N. Y. Jin, G. R. Booker, and I. R. Grant, Mater. Sci. Eng. Forum B **20**, 94 (1993).